https://doi.org/10.1142/9789811278952_0014

Chapter 14

Cryogenics for the HL-LHC

S. Claudet, G. Ferlin, E. Monneret, A. Perin, M. Sisti, R. Van Weelderen, A. Lees, V. Gahier, K. Brodzinski and L. Delprat

CERN, TE Department, Genève 23, CH-1211, Switzerland

The discovery of a Higgs boson at CERN in 2012 was the start of a major program working to measure this particle's properties with the highest possible precision for testing the validity of the Standard Model and to search for further new physics at the energy frontier. The LHC is in a unique position to pursue this program. Europe's top priority is the exploitation of the full potential of the LHC, including the high-luminosity upgrade of the machine and detectors with an objective to, by around 2030, collect ten times more data than in the initial design. To reach this objective, the LHC cryogenic system must be upgraded to withstand higher beam current and higher luminosity at top energy while keeping the same operation availability by improving the collimation system and the protection of electronics sensitive to radiation. This paper will present the conceptual design of the cryogenic system upgrade with recent updates in performance requirements, the corresponding layout and architecture of the system as well as the main technical challenges which have to be met in the coming years.

1. Overview

The upgrade of the cryogenics for the HL-LHC will consist of the following:

- design and installation of two new cryogenic plants at P1 and P5 for high luminosity insertions. This upgrade will be based on a new sectorization scheme aimed at separating the cooling of the magnets in these insertion regions from the arc magnets and considering the new feedboxes and superconducting links located in underground infrastructures.

- design and installation of a new cryogenic distribution lines (QXL) at P1 and P5 in the LHC tunnel and in a new underground service galleries.
- upgrade of the existing cryogenic plant (QSRA and QURA) cooling the LHC sector 3-4 located at P4.
- cryogenic design support for superconducting devices, such as magnets, crab cavities, superconducting links, and the hollow electron lenses.

Some other options such as new cryogenic circuits at P7 for the superconducting links and displaced current feedboxes or a new cryoplant in P4 have been discarded.

2. LHC Machine Upgrades

2.1. *Upgraded beam parameters and constraints*

The main parameters impacting the cryogenic system are given in Table 1. With respect to the nominal beam parameters, the beam bunch population will double and the luminosity in the detectors of the high luminosity insertions at P1 and P5 will be multiplied by a factor 5 with respect to LHC nominal luminosity.

These upgraded beam parameters will introduce new constraints to the cryogenic system:

- The collimation scheme must be upgraded. As some of the new collimators will work at room temperature but be installed on the cold region, cryogenic bypasses are required to guarantee the continuity of the cryogenic and electrical distribution.
- Hollow electron lenses will be installed for halo control.

Table 1. LHC upgraded beam parameters for 25ns bunch spacing.

Parameter	Unit	Nominal LHC	Nominal HL-LHC
Beam energy, E	TeV	7	7
Bunch population, N_b	protons/bunch	1.15×10^{11}	2.2×10^{11}
Number of bunches per beam, n_b		2808	2748
Luminosity, L	$cm^{-2}\ s^{-1}$	1×10^{34}	5×10^{34}
Bunch length	ns	1.04	1.04

- To improve the luminosity performance by addressing the geometric luminosity reduction factor and possibly allowing the levelling of the luminosity, cryo-modules of crab-cavities (CC) will be added at P1 and P5.

Finally, the matching and final focusing of the beams will require completely new insertion cryo-assemblies at P1 and P5.

3. Temperature Level and Heat Loads

Heat load to the cryogenic system have various origins and uncertainties. The heat loads deposited in the accelerator are the result of physical mechanisms, which are classified as static, resistive, beam-induced, collision-induced, or radiofrequency-induced. The nomenclature is based on the LHC Design Report [1].

An important effort has been done during the last years to estimate the future HL-LHC heat loads [2]. The heat loads values in Table 2 are categorized by temperature level and heat load type. Table 3 reports the heat load values for group of users. It indicates the total contribution from static, dynamic (nominal/ultimate), total load (nominal/ultimate) and design values.

Table 2. "Nominal heat load" table for the LSS.R5 for the HL-LHC. Preliminary values.

Component	Q1	Q2A	Q2B	Q3	CP	D1	Intercon.	DFX	DFM	D2	CC
Length (m) (thermal shield)	10.140 (10.640)	9.785	9.785	10.140	6.01 (6)	7.370	6.930 (6 unit *)	2.535 (3.034)	4.000	13.025 (14.025)	2 module units †
Cold Mass											
Temperature (K)	1.9	1.9	1.9	1.9	1.9	1.9	1.9	4.5	4.5	1.9	2
Total Heat Load (W)	138.9	122.7	157.5	163.9	97.4	97.1	38.2	4.1	4.5	46.7	89.9
Avg. Heat Load (W/m)	13.7	12.5	16.1	16.2	16.2	13.2	5.5 W pu	1.6	1.1	3.6	45.0 W pu
Static (W/m)	1.7	1.7	1.7	1.7	1.8	2.2	0.3 W pu	1.6	1.1	0.6	18.9 W pu
Resistive (W/m)	0.7	0.4	0.4	0.7	3.9	0.1	0.0 W pu	0.0	0.0	0.0	0.0 W pu
Beam Induced (W/m)	0.3	0.2	0.2	0.3	0.0	0.1	2.2 W pu	0.0	0.0	0.2	0.0 W pu
Collision Induced ‡ (W/m)	11.0	10.3	13.8	13.5	10.5	10.7	3.0 W pu	0.0	0.0	2.8	0.0 W pu
RF Cavity (W/m)	-	-	-	-	-	-	-	-	-	-	26.1 W pu

Table 2. (*Continued*)

Component	Q1	Q2A	Q2B	Q3	CP	D1	Intercon.	DFX	DFM	D2	CC
Beam Screen											
Temperature (K)	60-80	60-80	60-80	60-80	60-80	60-80	60-80	-	-	4.5-20	4.5-20
Total Heat Load (W)	223.1	97.3	144.8	133.0	66.9	74.0	375.8	0.0	0.0	49.8	46.0
Avg. Heat Load (W/m)	22.0	9.9	14.8	13.1	11.1	10.0	54.2 W pu	0.0	0.0	3.8	23.0 W pu
Static (W/m)	0.1	0.1	0.1	0.1	0.2	0.2	0.0 W pu	0.0	0.0	0.0	9.3 W pu
Resistive (W/m)	0.0	0.0	0.0	0.0	0.0	0.0	0.0 W pu	0.0	0.0	0.0	13.6 W pu
Beam Induced (W/m)	5.1	2.9	4.4	5.1	0.6	2.3	42.4 W pu	0.0	0.0	3.7	0.0 W pu
Collision Induced ‡ (W/m)	16.8	6.9	10.2	7.9	10.3	7.6	11.9 W pu	0.0	0.0	0.2	0.0 W pu
Thermal Shield											
Temperature (K)	60-80	60-80	60-80	60-80	60-80	60-80	60-80	60-80	60-80	60-80	60-80
Total Heat Load (W)	66.6	53.2	53.2	54.3	133.8	103.2	22.2	24.9	28.0	133.1	609.0
Avg. Heat Load (W/m)	6.3	5.4	5.4	5.4	22.2	14.0	3.2 W pu	8.2	7.0	9.5	304.5 W pu
Static (W/m)	6.3	5.4	5.4	5.4	22.2	14.0	3.2 W pu	8.2	7.0	9.5	206.9 W pu
RF Cavity (W/m)	-	-	-	-	-	-	-	-	-	-	97.6 W pu

"-" = not applicable; W pu = Watts per unit.
* Length of each interconnection unit is 1 m, except between Q3-CP which is 1.8 m and CP-D1 which is 1.13 m.
† A module unit contains 2 crab cavities.

Table 3. Total heat loads divided by group of users, LSS.R5 and IP5. Preliminary values.

Group*	IT	D2	CC	LSS_R5	IP5
Cold mass length (m)	62.7	17	-	79.7	159.4
Thermal shield length (m)	63.7	18	-	81.7	163.4
Number of units (-)	-	-	2	2(CC)	4(CC)
Cold Mass					
Temperature (K)	1.9	1.9	2	1.9-2	1.9-2
Total Design + flash (W)	1416.7	100.2	149.6	1667	3333
Total Design (W)	1173.3	83.0	127.6	1384	2768
Total Ultimate (W)	1103.4	68.7	89.9	1262	2524
Total Nominal (W)	779.4	50.7	89.9	920	1840
Dynamic - Ultimate (W)	1033.4	54.4	52.2	1140	2280
Dynamic - Nominal (W)	709.4	36.4	52.2	798	1596
Static (W)	70.0	14.3	37.7	122	244

Table 3. (*Continued*)

Group*	IT	D2	CC	LSS_R5		IP5	
Beam Screen							
Temperature (K)	60-80	4.5-20	4.5-20	60-80	4.5-20	60-80	4.5-20
Total Design (W)	1685.0	74.7	97.0	1685	172	3367	343
Total Ultimate (W)	1424.1	50.9	46.0	1424	97	2846	194
Total Nominal (W)	1115.0	49.8	46.0	1115	96	2228	192
Dynamic - Ultimate (W)	1415.8	50.9	27.3	1416	78	2830	156
Dynamic - Nominal (W)	1106.7	49.8	27.3	1107	77	2211	154
Static (W)	8.4	0.0	18.7	8	19	17	37
Thermal Shield							
Temperature (K)	60-80	60-80	60-80	60-80		60-80	
Total Design (W)	744.9	229.6	913.5	1967		3935	
Total Ultimate (W)	496.6	153.1	609.0	1312		2623	
Total Nominal (W)	496.6	153.1	609.0	1312		2623	
Dynamic - Ultimate (W)	0.0	0.0	195.2	195		390	
Dynamic - Nominal (W)	0.0	0.0	195.2	195		390	
Static (W)	496.6	153.1	413.8	1116		2233	

(*) *italic* values are indicating Design Heat Load values

The design heat load values consider margins and technological requirements. They can be calculated by using the following equations:

$$\dot{Q}_{\text{installed}} = \text{MAX}\left[F_{ov} \cdot \left(F_{un} \cdot \dot{Q}_{\text{static}} + \dot{Q}_{\text{dynamic nominal}}\right) ; F_{un} \cdot \dot{Q}_{\text{static}} + \dot{Q}_{\text{dynamic ultimate}}\right] \quad (1)$$

$$\dot{Q}_{\text{installed}} = \text{MAX}\left[F_{ov} \cdot \dot{Q}_{\text{nominal}} ; \dot{Q}_{\text{ultimate}}\right] \quad (2)$$

Equation (1) is valid for the cold mass (1.9–2 K) and beam screens (4.5–20 K and 60–80 K). Equation (2) is valid for the thermal shield (60–80 K) and current leads (20–293 K). A detailed study is available on Fig. 1 which gives a global view of the heat load at 1.9 K.

4. Impact on Existing Sector Cryogenic Plants

With new cryogenic plants dedicated to the cooling of cryogenic equipment in P1 and P5, the cooling duty of the existing sector cryogenic plants will be

reduced and more equally distributed. Figures 2 and 3 show the required cooling capacities for the different temperature levels and compares them to the nominal cooling requirements and to the installed capacities (green bars).

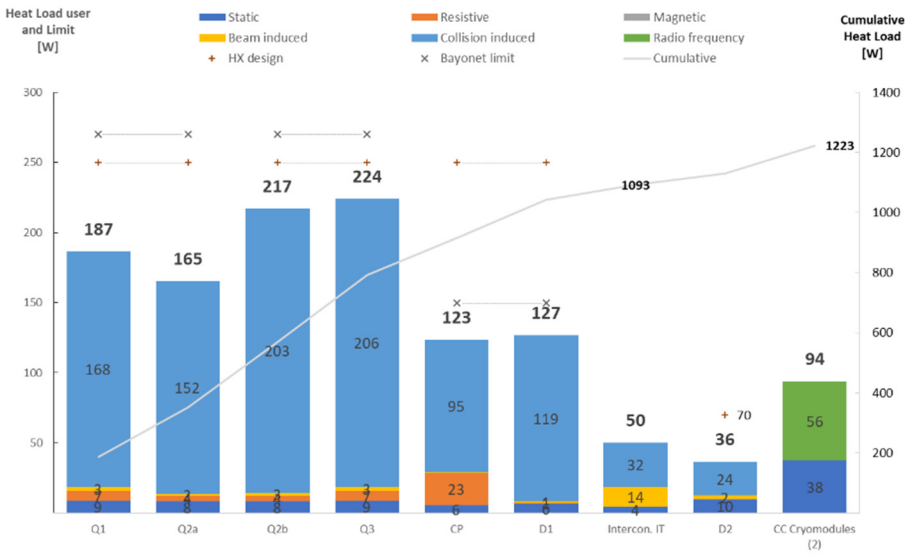

Fig. 1. Total heat load for users at 1.9 K. Preliminary values.

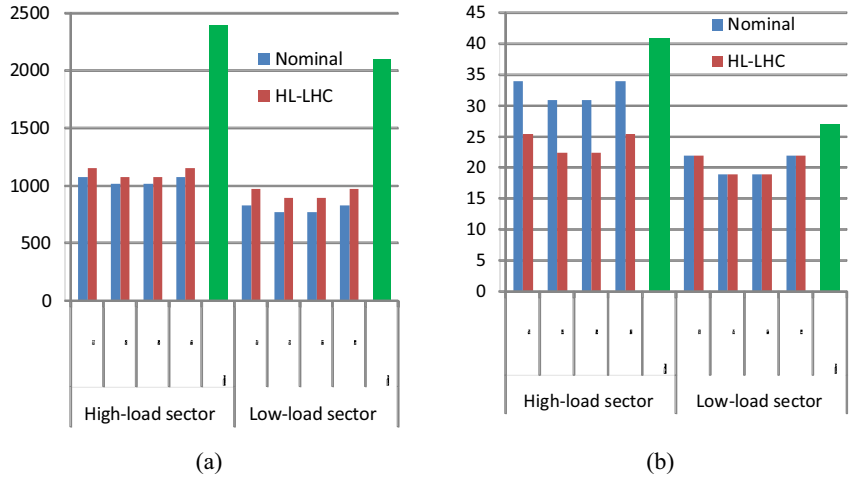

(a) (b)

Fig. 2. Cooling capacity requirement of sector cryogenic plants: (a) cold mass; (b) current leads.

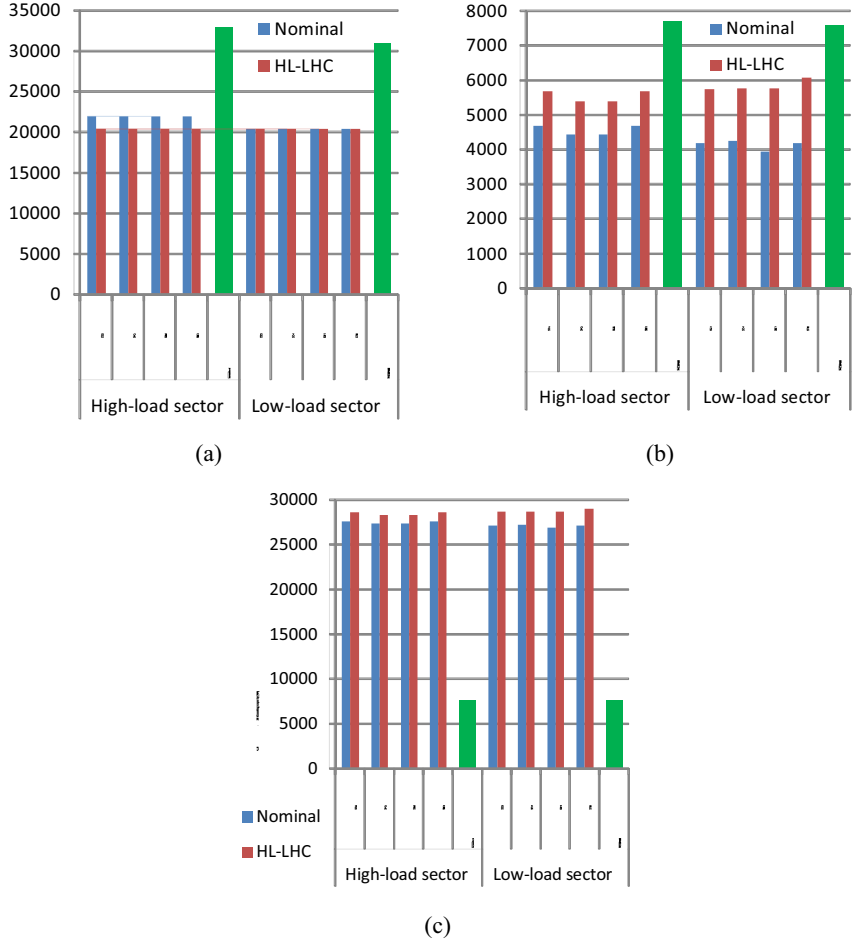

Fig. 3. Cooling capacity requirement of sector cryogenic plants: (a) thermal shields; (b) beam screen (dipole off); (c) beam screen (dipole on).

The low-load sectors equipped with upgraded ex-LEP cryogenic plants have lower installed capacity than the four cryogenic plants specially ordered for the LHC high-load sectors. For the HL-LHC, sufficient capacity margin still exists provided that the beam scrubbing of dipole beam-screens is efficient (dipole off).

5. Point 4 Cryogenics

The initial baseline considered the installation of a new cryoplant in P4. Later on, it was decided to evaluate an alternative scenario for the refrigeration part. The alternative scenario consisted of an upgrade of one of the existing refrigerators of P4 (equivalent of 2 kW@4.5 K with respect to the existing plant capacity of 16.5 kW@4.5 K) to fulfil the required cooling capacity of existing SRF modules with sufficient margin, while keeping or adapting the distribution system depending on the alternative. As a complement, a new mobile refrigerator with a cooling capacity allowing RF tests of a single cryomodule during long shut-downs was then considered, as all other cryogenic sub-systems would be stopped for maintenance and major overhauling but was finally abandoned.

The upgrade of the ex-LEP refrigerator included mainly:

- Replacement of 7 expansion turbines.
- Modification of one existing turbine.

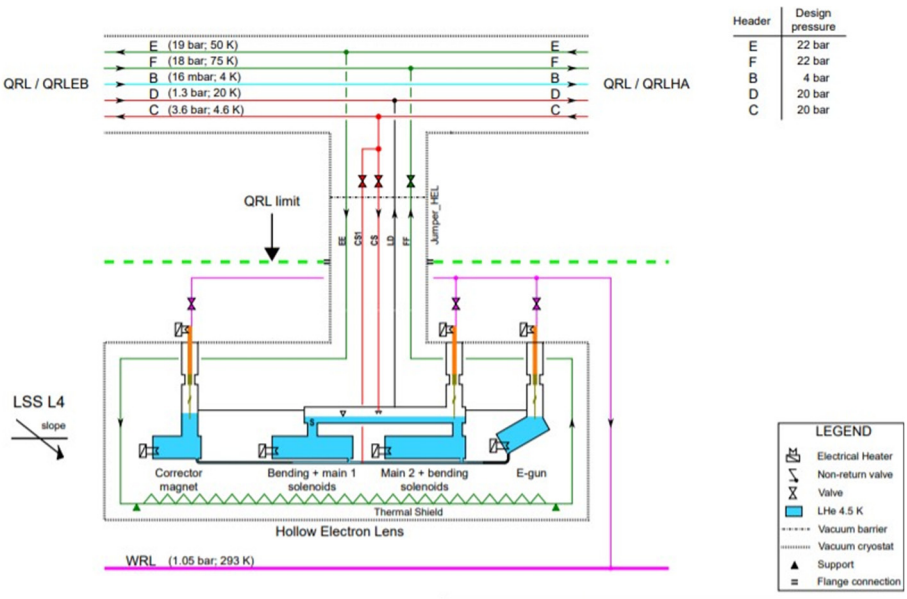

Fig. 4. Layout of the possible cryogenic layout at P4 (Hollow e-lens).

- Modification of the required piping inside the boxes or for instrumentation and service panels.

The upgrade was successfully completed during the Long Shutdown 2.

The modification of the cryogenic distribution line to allow the installation of the hollow electron lenses is under study. The schematic layout can be seen in Figure 4 [5].

6. New Cryogenics for High Luminosity Insertions at Point 1 and Point 5

The new HL-LHC cryogenic system will require new cryo-plants of about 15 kW at 4.5 K including 3 kW at 1.8 K. They will encompass new refrigeration plants and distribution lines. Figure 5 illustrates the architecture of the system. A full analysis of both systems has been done in order to optimize the cost and the sourcing strategy.

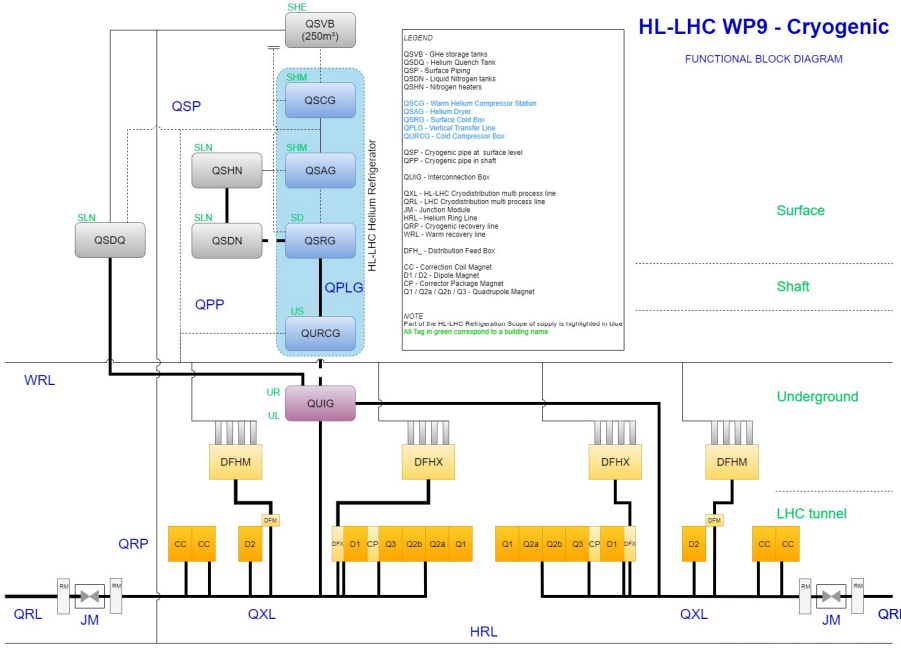

Fig. 5. HL-LHC Cryogenic architecture at P1 and P5.

The main components of the new helium refrigeration system are [7]:

- the compressor station (QSCG)
- a dryer system (QSAG)
- the 4.5 K cold box (QSRG) including 80 K and 20 K absorbers and a liquid helium phase separator
- a cryogenic vertical transfer line (QPLG) in a shaft connecting the 4.5 K surface cold box to the 1.8 K cold box located in an underground cavern
- a 1.8 K cold box (QURCG) including the cold compressors and a phase separator.

Each HL-LHC helium refrigerator shall:

- provide cooling to different magnets with an equivalent capacity of about 3 kW at 1.8 K
- supply an average helium mass flow rate of approximatively 10 g/s at 4.5 K for the beam screens and recover it at around 20 K
- provide cooling to the Distribution Feed Boxes (DFH) with a liquefaction flow rate of 25 g/s
- supply an average helium mass flow rate of approximatively 100 g/s at 60 K for various thermal shields and recover it at around 80 K, for a corresponding cooling capacity of 10 kW
- allow control of supply temperature between 300 K and 10 K during cool down of magnets
- accommodate heat load variation from 20 to 100% in less than one hour twice a day.

Regarding the new distribution system, it shall:

- distribute helium from the refrigerator to the different machine components in the temperature range from 4 K to 350 K with a maximum allowable pressure of 25 bar absolute
- control the helium flow to and from users as required for multiple operating modes
- have a maximum heat load for lines below 20 K ($Ø_{eq} \sim 320$ mm) lower than 0.4 W/m
- have a vacuum vessel diameter ranging from ~650 mm to ~770 mm
- house five inner headers ranging from ISO DN40 to DN300 and an actively cooled thermal shield

- integrate approximately 200 cryogenic control valves and interface to users via 32 feeding points.

Figure 6 illustrates the cryogenic distribution architecture while the following details provide details on the layout for the different components.

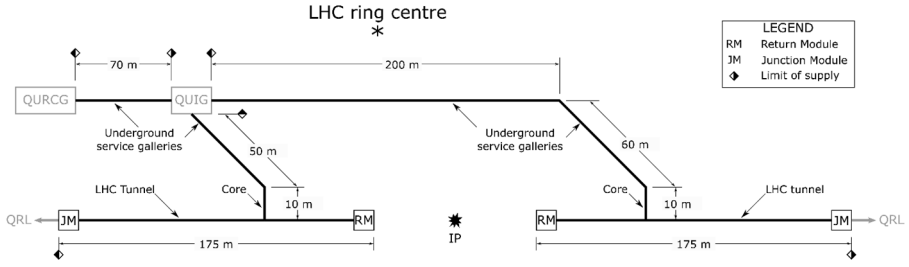

Fig. 6. Schematic of the cryogenic distribution architecture [8].

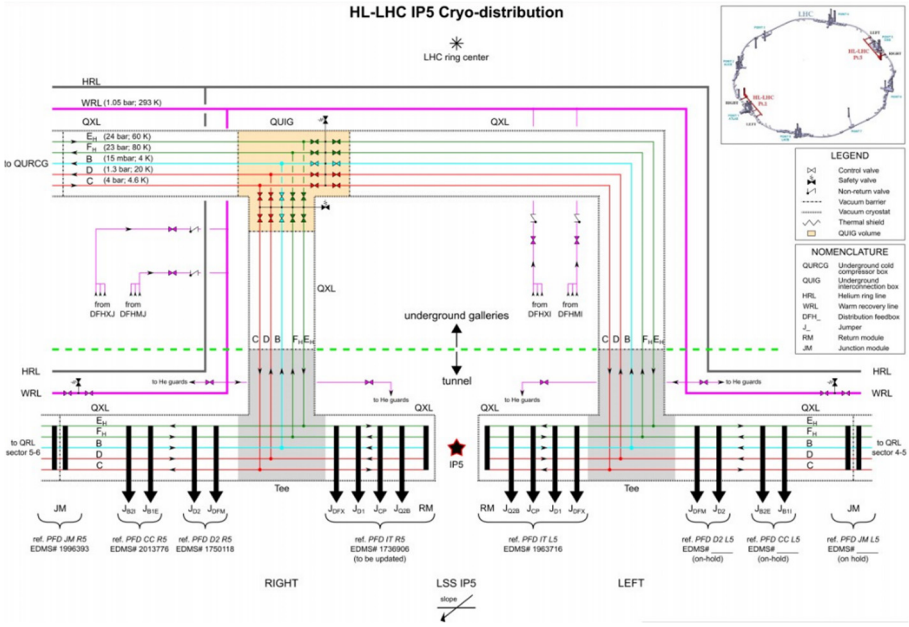

Fig. 7. Layout of the IP5 Cryodistribution [9].

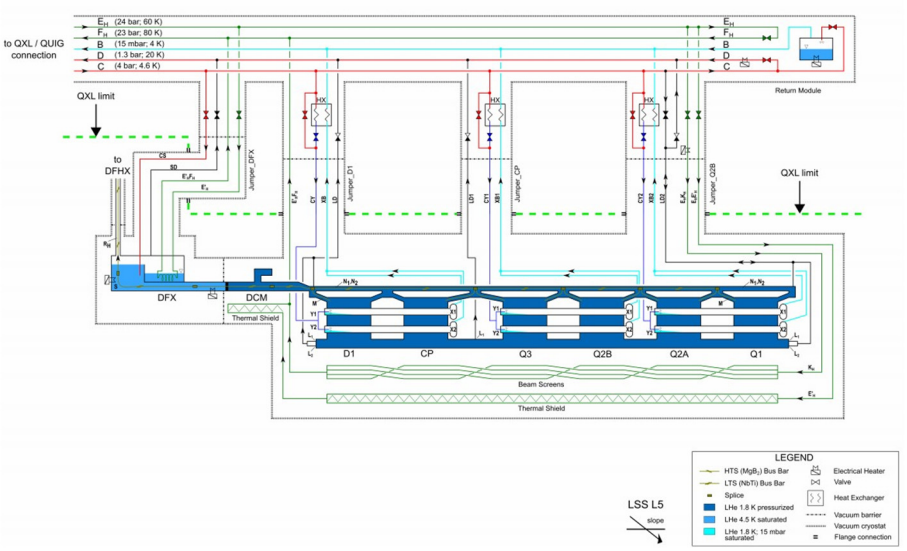

Fig. 8. Detail of the distribution for the IT magnets, CP and D1 [10].

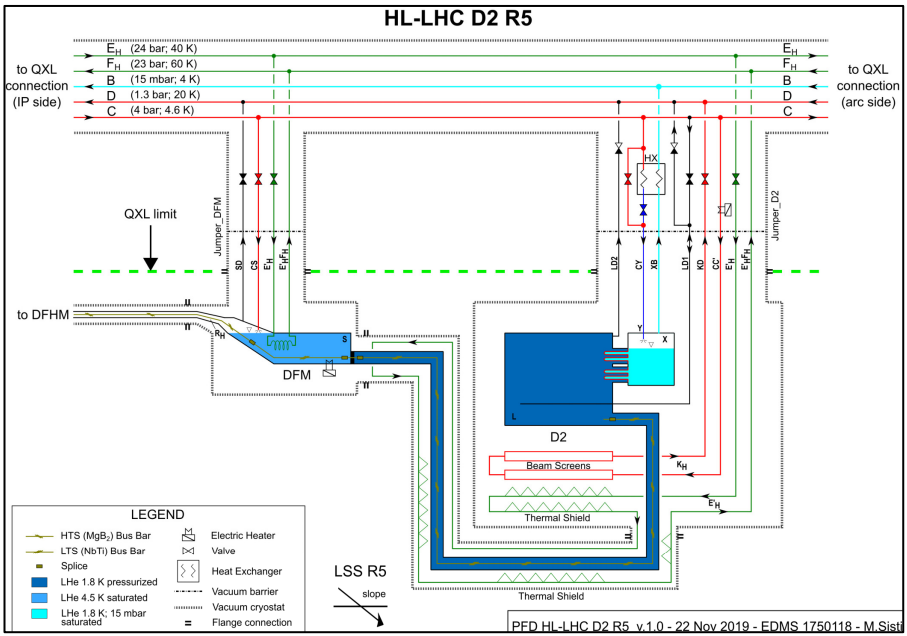

Fig. 9. Detail of the distribution for the D2 magnet [11].

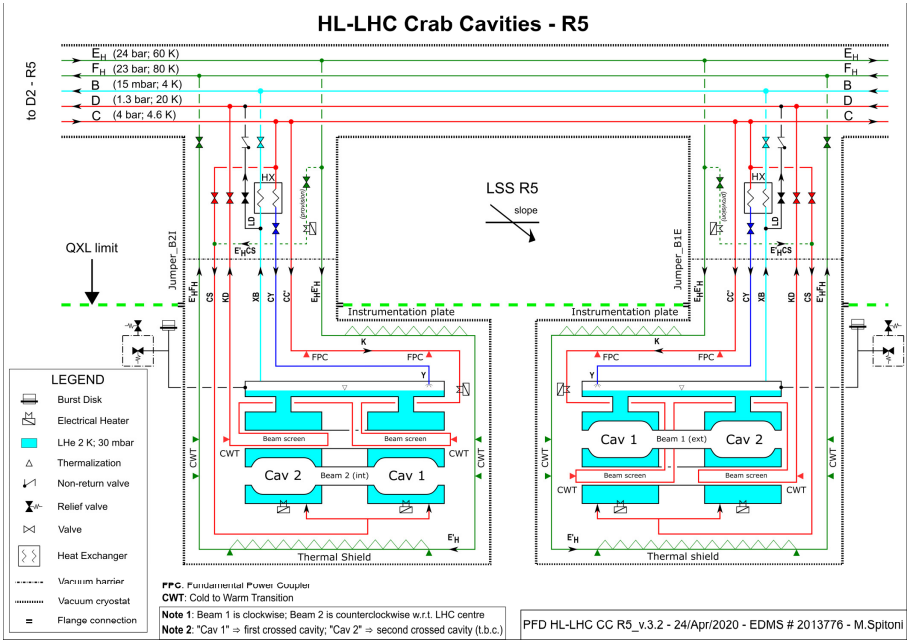

Fig. 10. Detail of the distribution for the Crab Cavities [12].

References

1. J. Poole, LHC Design Report Volume I., The LHC Main Ring, Chapter 11, CERN, (2004). EDMS: https://edms.cern.ch/document/445856.
2. V. Gahier, U. Wagner and P. Zijm, Heat load definition for the HL-LHC project, Updated heat load tables for the LSS.R5 for the HL-LHC. EDMS: https://edms.cern.ch/document/1610730.
3. M. Sisti, Process flow diagram of the HL-LHC IT L5. EDMS: https://edms.cern.ch/document/1963716.
4. M. Sisti, Cryo distribution IP5. EDMS: https://edms.cern.ch/document/2025508.
5. M. Spitoni, Process Flow Diagram of HL-LHC Hollow e-Lens in L4. EDMS: https://edms.cern.ch/document/2314734.
6. E. Monneret, IT-4472 Upgrade of the ex-LEP Refrigerator for HL-LHC - Point 4. EDMS: https://edms.cern.ch/document/2001440.
7. E. Monneret, MS-4631 - Supply of Two New Helium Refrigerators for HL-LHC at Point 1 (P1) and Point 5 (P5). EDMS: https://edms.cern.ch/document/2382454.
8. M. Sisti, MS-4630 - Supply of the Cryogenic Distribution Lines for the HL-LHC at Point 1 (P1) and Point 5 (P5). EDMS: https://edms.cern.ch/document/2381328.

9. M. Sisti, Process flow diagram of HL-LHC IP5. EDMS: https://edms.cern.ch/document/2025508.
10. M. Sisti, Process flow diagram of HL-LHC IT L5. EDMS: https://edms.cern.ch/document/1963716.
11. M. Sisti, Process flow diagram of HL-LHC D2 R5. EDMS: https://edms.cern.ch/document/1750118.
12. M. Spitoni, Process flow diagram of HL-LHC Crab Cavities R5. EDMS: https://edms.cern.ch/document/2013776.
13. V. Gahier, Process flow diagram of HL-LHC DFX/DSHX/DFHX L5. EDMS: https://edms.cern.ch/document/2322140.